# Thermal Property Characterization of a Low Supercooling Degree Binary Mixed Molten Salt for Thermal Energy Storage System

Y. Li[1] · C. G. Wang[1] · G. Y. Liu[2] · Q. Z. Zhu[1] · Z. Z. Qiu[1]

## Abstract

In this paper, $LiNO_3$–NaCl binary mixed molten salt with high phase change enthalpy was selected as phase change materials (PCM). $LiNO_3$ was used as the main phase change material, and NaCl was used as the additional material to change the properties and reduce the supercooling degree of molten salts. $LiNO_3$–NaCl binary mixed molten salts with different mass proportion were prepared by static melting method. The optimum eutectic ratio of the mixed molten salt was obtained through analysis of the experiment results. The influence of NaCl on phase change temperature, decomposition temperature, supercooling degree and phase change latent heat were tested and analyzed. The properties of the phase change materials were characterized by thermogravimetric analyzer and simultaneous differential scanning calorimeter (TGA/DSC), scanning electron microscopy (SEM) and X-ray diffraction (XRD). The phase transition temperature, latent heat and supercooling degree of the binary mixed molten salts showed nonlinear variation with the increase in NaCl mass fraction. When the mass ratio was 88:12 for $LiNO_3$–NaCl, the phase change temperature was the lowest of 222.6 °C, the phase change latent heat was the highest of 389.3 $J \cdot g^{-1}$ and the supercooling degree was 1.2 °C. The optimum eutectic crystallization degree was achieved. At the same time, the decomposition temperature of the mixed molten salt was increased from 560 °C to 620 °C with the addition of NaCl, which greatly increased the applicable temperature range of $LiNO_3$.

**Keywords** $LiNO_3$–NaCl binary phase change material · Low supercooling degree · Morphological characterizations · Thermal characterization

✉ Q. Z. Zhu
zhuqunzhi@shiep.edu.cn

1    College of Energy and Mechanical Engineering, Shanghai University of Electric Power, Shanghai 200090, China

2    Shanghai Zibao Residential Industry Co., Ltd, Shanghai 310000, China

## 1 Introduction

Solar energy is an infinite and environment-friendly energy source, but solar energy is always characterized as unstable and cyclic. Energy storage is an essential technology to mitigate the instability and time discrepancy between solar energy supply and energy demand [1]. Industrial waste heat is divided into three categories by temperature. According to the second law of thermodynamics, the medium temperature waste heat (120 °C to 300 °C) and low temperature waste heat (< 120 °C) are hard to be recycled [2]. Heat storage is an effective way to utilize them.

The thermal storage technology mainly includes chemical heat storage, sensible heat storage and phase change heat storage. Phase change thermal storage technology is known by scholars [3–7] for its large heat storage density, small temperature change during the heat absorption and heat release processes.

The melting point of inorganic salt phase change materials is between 100 °C and 1000 °C. They usually have a relatively high phase change latent heat. They are used as the medium and high-temperature phase change thermal storage material. Among them, $CaCl_2$, KCl, $NaNO_3$, $KNO_3$, $LiNO_3$, $FeCl_3$, $Na_2Si_2O_5$, $Na_2SO_4$, NaCl, NaOH and KOH are most widely used [8]. One of the main problems of using them is supercooling degree due to weak nucleating properties. G. Lane [9] pointed out that this supercooling effect is not acceptable because it reduces the utility of the material, and if too severe, could completely prevent heat recovery. Many factors determine whether an additive can promote nucleation [10].

There are various chlorates with the phase change temperature of 100 °C to 800 °C. They usually have high specific heat capacity and phase change latent heat, better thermal stability and high thermal conductivity, but generally they are strongly corrosive. Myers et al. [11] did a preliminary survey of chloride salts and binary eutectic systems, and the result showed that they are promising high-temperature thermal storage materials. Arconada [12] pointed out that NaCl had a low cost and was abundant. They produced the macro-encapsulation of sodium chloride with detailed structural and thermophysical characterization. Yang [13] added various proportions of NaCl/NaCl solution into the n-octadecane-based PCMs for thermal energy storage. The experimental results showed that 20 wt% NaCl solution has the greatest effect on the thermal performance. The supercooling degree had been minimized up to 6 °C with the addition of NaCl. Liao et al. [14] prepared $Na_2CO_3$–$KCO_3$ mixed molten salt and added high melting point material of NaCl, KCl, $Li_2CO_3$ to modify the material property. The results showed that $Na_2CO_3$–$KCO_3$–NaCl has outstanding performance. The melting point lowered to 133 °C, and phase change latent heat increased to 1.9 times compared to $Na_2CO_3$–$KCO_3$. The thermal property kept stable under 850 °C. It was a kind of ideal high-temperature heat carrier. Gasanaliev et al. [15] analyzed the mixed molten salt of nitrate and chloride. They found that chloride could reduce the phase change temperature and kept the high phase change latent heat.

The phase change temperature of nitrate mixed molten salt is about 120 °C to 300 °C. Nitrates have excellent heat transfer and flow characteristics, and it is easy to be eutectic with other inorganic salt. It is the most common phase change thermal storage medium. Many scholars studied their thermal physical performance decades ago. Peng et al. [16] prepared a new kind of cheaper quaternary mixed molten salt of

**Table 1** Experimental materials

| Name | Type | Melting temperature (°C) | Latent heat ($J \cdot g^{-1}$) | Manufacturer |
|------|------|--------------------------|--------------------------------|--------------|
| $LiNO_3$ | (AR $\geq$ 99.0 %) | 255 | 362 | Shanghai Feng shun Chemical Co., Ltd |
| NaCl | (GR $\geq$ 99.9 %) | 801 | 492 | Sinopharm Chemical Reagent Co., Ltd |

K, Na/$NO_2$, Cl, $NO_3$. The mixed molten salt has a low melting point of 140 °C and could keep good thermal stability under 500 °C. Tamme et al. [17] studied the working pressure system of $KNO_3$–$NaNO_3$, $KNO_3$–$NaNO_3$–$NaNO_2$ and the expanded graphite composite mixed molten salt. Xu et al. [18] fabricated sodium nitrate-based diatomite composite materials and studied their thermal and physical properties. Li et al. [19, 20] prepared 40 % $LiNO_3$–60 % $KNO_3$ binary molten salt nitrate with excellent thermal stability. The melting point was 131.3 °C, and phase change latent heat was 170.2 $J \cdot g^{-1}$. The three mixed molten salts (60 % $NaNO_3$ + 40 % $KNO_3$, 7 % $NaNO_3$ + 53 % $KNO_3$ + 40 % $NaNO_2$, 7 % $NaNO_3$ + 45 % $KNO_3$ + 48 % $Ca(NO_3)_2$) have been used in heat storage, heat transfer and related industrial processes as the commercialized energy storage materials from decades ago [21, 22].

In this paper, $LiNO_3$ with the high latent heat value and medium phase change temperature was chosen as the basal phase change material. NaCl was added to change the performance and lower the supercooling degree. $LiNO_3$–NaCl binary mixed molten salt with different mass ratios were prepared and analyzed. The test results were compared with FactSage computational result [23]. Thermal property, crystallization and supercooling degree of the material were studied.

## 2 Materials and Methods

### 2.1 Preparation of Materials

$LiNO_3$ and NaCl were used as raw materials to prepare the binary mixed molten salt, and the raw material information is shown in Table 1. In this paper, the melting point and phase change latent heat of the raw materials were tested by TGA/DSC. The test results were almost the same with the references. The values shown in Table 1 are the measured values.

The binary mixed molten salt was prepared using static mixing melting method. $LiNO_3$ and NaCl in powder state were placed in a constant temperature air blast oven (120 °C) for drying 24 h. $LiNO_3$ and NaCl at different mass ratios were placed in the ball milling tanks for 1 h grinding at the speed of 500 RPM. They were then put

in muffle furnace to be heated up to 400 °C at the heating rate of 5 °C·min$^{-1}$ and stayed for 120 min. The samples were cooled in the furnace to about 150 °C; then, they were taken out to cool in the air to room temperature. The block mixed molten salts were taken from the corundum crucible. $LiNO_3$–NaCl binary mixed molten salts were obtained after grinding and drying.

## 2.2 Characterization Techniques

### 2.2.1 Phase Analysis

In this paper, the sample preparation process includes physical mixing, high temperature melting, etc. It is necessary to analyze the sample composition to determine whether there are reactions between experimental samples or between the crucible container and experimental samples. XRD test used D/Max–2550VB/PC type X-ray diffractometer (Rigaku company, Japan). CuKα was used as a radiation source, the wavelength was 0.15406 nm, and scan angle was 10°–90°.

### 2.2.2 Morphological Analysis

Crystal morphology of binary mixed molten salt was tested and analyzed by scanning electron microscope (SEM, JXL30 FE, FEI company, the United States). The samples were deposited on the specimen holder by glue carbon belt. The samples were sprayed with gold to form a gold film layer, which helped to clearly observe the morphology of the samples. Specimen holder was placed on the corresponding position of the instrument. They were vacuumed firstly and then selected, scanned and photographed.

### 2.2.3 Phase Change Behavior Analysis

Thermogravimetry and differential scanning calorimeter is a kind of apparatus which can complete TG and DSC analysis at the same time using the same sample. In this article, METTLER TGA/DSC2 1600LF (Mettler-Toledo company, Switzerland) thermal analyzer was chosen to analyze the thermal properties of the prepared phase change materials. Phase change temperature, phase change latent heat and specific heat were tested for $LiNO_3$ and $LiNO_3$–NaCl with different mass ratios (94:6, 88:12, 80:20). The volume of the alumina crucible is 50 ml, calorimeter measurement precision is within $\pm 0.5$ % and temperature measurement precision is about $\pm 0.3$ K.

Because $LiNO_3$–NaCl binary mixed molten salt is easily deliquescent, it is necessary to put the test samples inside a constant temperature air blast oven at 120 °C for 24 h to reduce the influence of moisture. The sample mass for test was between 5 mg and 20 mg, which can ensure the accuracy of test results and at the same time avoid the sample overflowing from the crucible after melting. For phase change temperature and latent heat test, the temperature range was 100 °C to 300 °C to 100 °C with the heating and cooling rate of 10 °C·min$^{-1}$. The temperature was kept at 300 °C for 5 min. Nitrogen gas was used as the protection gas with the flow rate of 20.0 ml·min$^{-1}$. For specific heat test, the temperature range was 100–350 with the heating and cooling
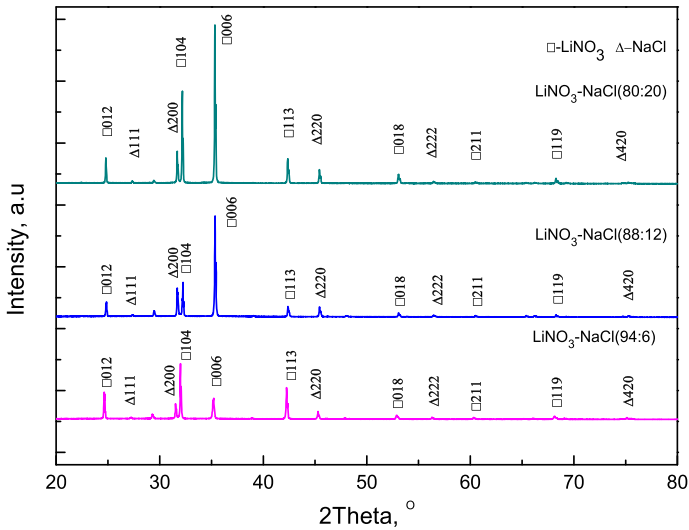
**Fig. 1** XRD diagram of $LiNO_3$–NaCl

rate of 10 °C·min$^{-1}$. Nitrogen gas was used as the protection gas with the flow rate of 20.0 ml·min$^{-1}$.

### 2.2.4 High-Temperature Heat Stability Test

The high-temperature heat stability test was done for $LiNO_3$ and 88 wt% $LiNO_3$–12 wt% NaCl. Test temperature range was 100 °C to 800 °C with the heating rate of 10 °C·min$^{-1}$. Nitrogen was used as protective gas with the flow velocity of 20 ml·min$^{-1}$.

## 3 Results and Discussion

### 3.1 XRD Test Results

XRD test results are shown in Fig. 1 for $LiNO_3$–NaCl binary mixed molten salt with NaCl at the mass fraction of 6 %, 12 %, 20 %, respectively. The main peak intensity of $LiNO_3$ (012), (104), (006), (113), (018) decreases at first and then increases with the increase in NaCl addition ratio. The main peak intensity of $LiNO_3$ is the minimum for 88 wt% $LiNO_3$–12 wt% NaCl. The main peak intensity of NaCl (200), (220) increases with the increase in NaCl mass ratio. The peak intensity can show the relative crystallization degree. For the sample with 12 wt% NaCl, the relative intensity difference of $LiNO_3$ and NaCl in the two groups (peaks (200) and (104), (220) and (113)) is minimum. It illustrates that mutual melting crystallization effect of $LiNO_3$ and NaCl is the best in all the three kinds of samples. The results are consistent with FactSage calculation results [23].
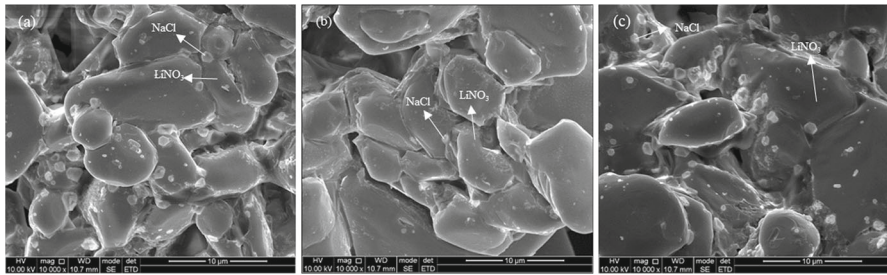
**Fig. 2** SEM images of LiNO$_3$–NaCl. (a) 6 wt% NaCl, (b) 12 wt% NaCl, (c) 20 wt% NaCl

### 3.2 SEM and EDS Microstructural Analysis

Figure 2 shows crystal surface SEM electron microscope scanning images of binary mixed molten salt with NaCl at the mass fraction of 6 %, 12 %, 20 %, respectively. The samples are observed under $5000 \times$, $10\,000 \times$ magnification. It can be seen clearly that some regular multilateral cubes attached to the crystal bed surface for the mixed molten salt with NaCl at the mass fraction of 6 % and 20 %. The crystal surface is the smoothest for the mixed molten salt with NaCl at the mass fraction of 12 %. Almost no exposed crystal structure can be seen.

Figure 3 shows the EDS images for the three kinds of mixed molten salts. The positions of the elements of Cl and Na can be seen from SEM electron microscope scanning images. It can be seen that the multilateral cube structure exposed in the crystal surface is NaCl. It can be concluded that NaCl and LiNO$_3$ mutually melt well and the crystallization effect is the best for 88 wt% LiNO$_3$–12 wt% NaCl.

### 3.3 Phase Change Behaviors of LiNO$_3$–NaCl PCM

The melting and freezing DSC curves of LiNO$_3$–NaCl binary mixed molten salts are shown in Fig. 4. The heating process is represented with the positive heat flow, and the cooling process is represented with the negative heat flow. The line between the starting point and the ending point of the peak is the baseline. In general, the phase transition temperature $T_m$ of phase change material is the intersection point of the tangent from start edge inflexion point and the baseline. Similarly, the corresponding freezing temperature is $T_s$.

$T_{peak-m}$ and $T_{peak-s}$ are the peak temperatures of endothermic and exothermic curves, respectively. The endothermic melting rate and exothermic crystallization rate peak at $T_{peak-m}$ and $T_{peak-s}$. The phase change enthalpy of phase change material is determined according to temperature–heat flux density curve. The area surrounded by endothermic peak and baseline is the melting enthalpy $H_m$. The area surrounded by exothermic peak and baseline is solidification enthalpy $H_s$. In general, the melting enthalpy is considered as phase change latent heat of mixed molten salt. The melting and crystallization properties of the samples are obtained from DSC analysis and are summarized in Table 2. The error analysis is as shown in Table 3.
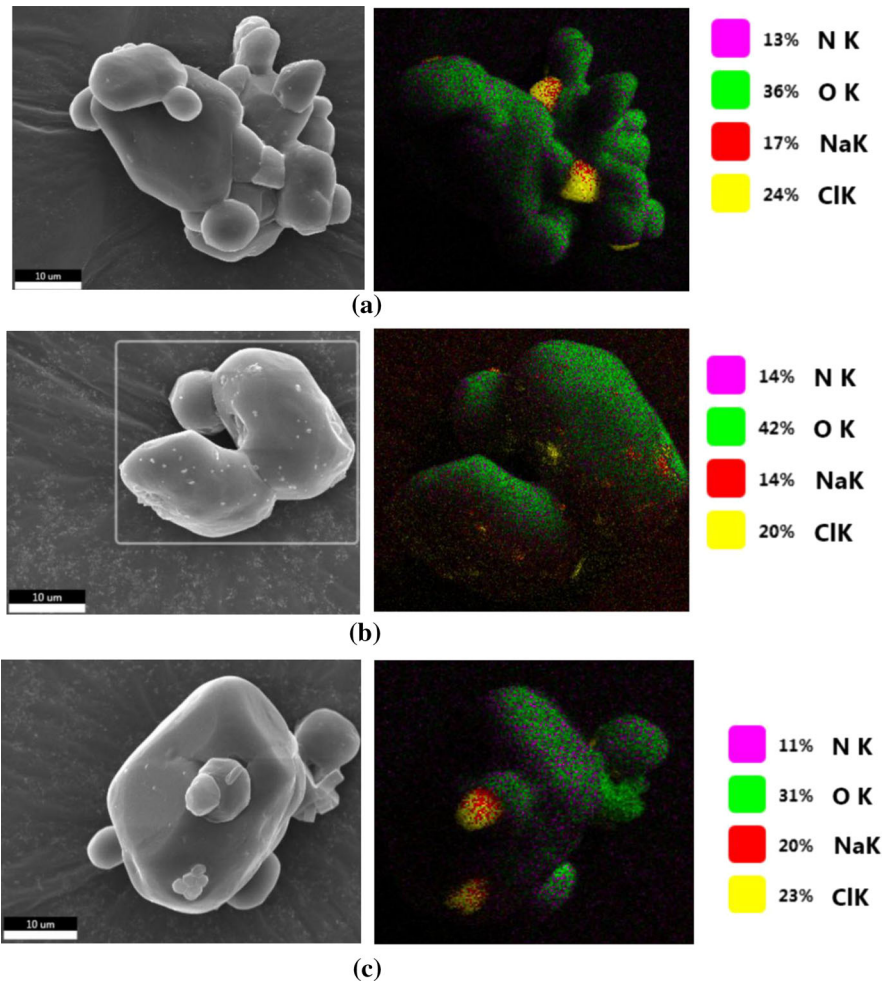
**Fig. 3** EDS images of LiNO$_3$–NaCl. (a) 6 wt% NaCl, (b) 12 wt% NaCl, (c) 20 wt% NaCl

It can be seen from Fig. 4 that the phase change temperature of LiNO$_3$ is 254.9 °C. The peak temperature of endothermic peak $T_{peak-m}$ is 263.5 °C, and the melting phase change latent heat $H_m$ is 362.2 J·g$^{-1}$. The phase change temperature of 12 wt% NaCl–88 wt% LiNO$_3$ is 223.6 °C, which reduces by 31 °C than pure LiNO$_3$. But the melting temperature increases with the further increase in NaCl mass ratio.

NaCl as heterogeneous salt plays the role of heterogeneous nucleation [24, 25]. The increase in the nucleation points makes the particle size decrease, thus the melting temperature of the mixed molten salt reduces. The melting phase change latent heat reaches the highest of 389.3 J·g$^{-1}$ for 88 wt% LiNO$_3$–12 wt% NaCl. The melting latent heat reduces with the further increase in NaCl mass ratio.

In the DSC endothermic curve of 94 wt% LiNO$_3$–6 wt% NaCl, there are two endothermic peaks. The first peak corresponds to the melting of NaCl–LiNO$_3$ binary
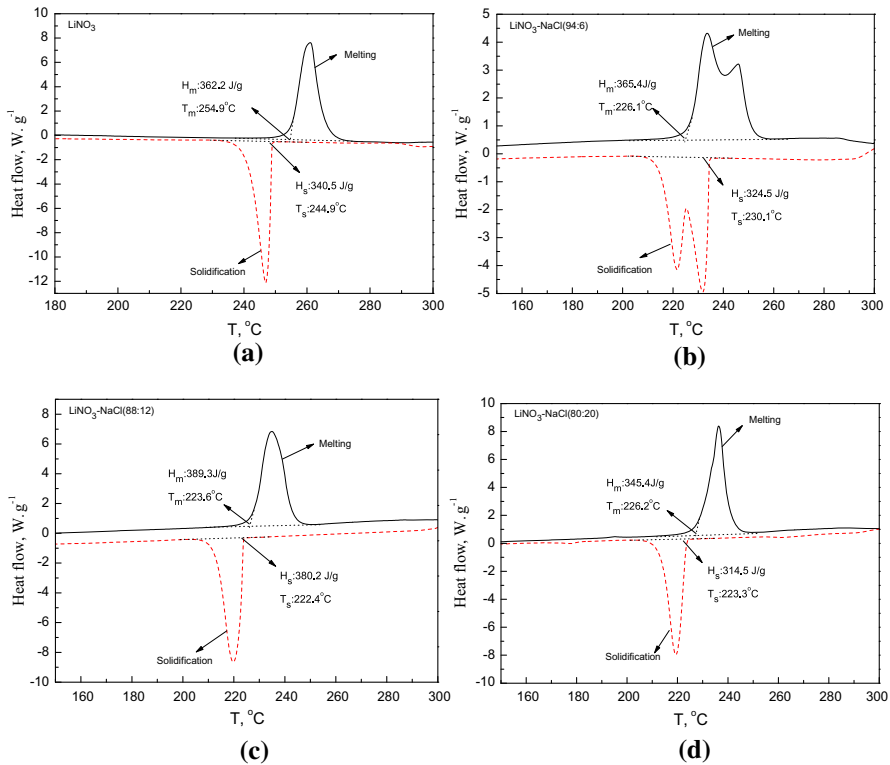
**Fig. 4** DSC curves of LiNO₃–NaCl with different mass ratios. (a) LiNO₃, (b) LiNO₃/NaCl (94:6), (c) LiNO₃/NaCl (88:12), (d) LiNO₃/NaCl (80:20)

**Table 2** DSC test results of LiNO₃–NaCl with different mass ratios

| Mass rate | $T_m$ (°C) | $T_{peak-m}$ (°C) | $H_m$ (J·g$^{-1}$) | $T_s$ (°C) | $T_{peak-s}$ (°C) | $H_s$ (J·g$^{-1}$) | Supercooling degree (°C) |
|---|---|---|---|---|---|---|---|
| 100:0 | 254.9 | 263.5 | 362.2 | 244.9 | 247.3 | 340.5 | 10 |
| 94:6 | 224.7 | 233.2 | 365.4 | – | – | 324.5 | – |
| 88:12 | 223.6 | 235.1 | 389.3 | 222.4 | 220.0 | 380.2 | 1.2 |
| 80:20 | 226.2 | 236.3 | 345.4 | 223.3 | 219.8 | 314.5 | 2.9 |

eutectic mixture, and another peak is the interaction result of LiNO₃ melting process and the residue contribution of the first peak. Supercooling degree is the difference of material melting temperature $T_m$ and crystallization temperature $T_s$. The addition of NaCl reduces the melting temperature of mixed molten salt. The supercooling degree of LiNO₃–NaCl reduces to 1.2 °C for 88 wt% LiNO₃–12 wt% NaCl, which basically can be ignored.

Supercooling is a common phenomenon in crystallization. Metastable state around the melting point can affect the crystallized process significantly. The addition of NaCl

**Table 3** Error analysis of DSC test results

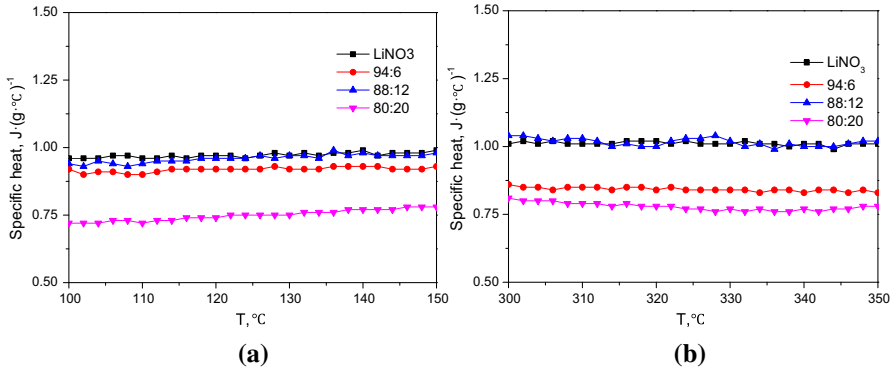| Mass rate | $\Delta T_m$ (°C) | $\Delta H_m$ (J·g$^{-1}$) | $\Delta T_s$ (°C) | $\Delta H_s$ (J·g$^{-1}$) |
|---|---|---|---|---|
| 100:0 | ±0.3 | ±1.8 | ±0.3 | ±1.7 |
| 94:6 | ±0.3 | ±1.8 | – | ±1.6 |
| 88:12 | ±0.3 | ±1.9 | ±0.3 | ±1.9 |
| 80:20 | ±0.3 | ±1.7 | ±0.3 | ±1.6 |



**Fig. 5** The specific heat curves with temperature change (a) solid state (b) liquid state

converts the crystallization from homogenous nucleation to heterogeneous nucleation. The nucleation points increase, and the nucleation barrier is reduced around the melting point. It accelerates the crystallized process and shortens the degree of supercooling.

For LiNO$_3$–NaCl binary mixture molten salt, there is a best eutectic ratio. According to the test results, 88 wt% LiNO$_3$–12 wt% NaCl has the best thermal physical performance and the lowest supercooling degree. Its melting temperature decreases by 31 °C than that of LiNO$_3$. The melting phase change latent heat increases by 27.1 J·g$^{-1}$ and the latent capacity increases by 7.5 %. The addition of NaCl helps to decrease phase change temperature and increase the phase change latent heat and improves the performance of LiNO$_3$.
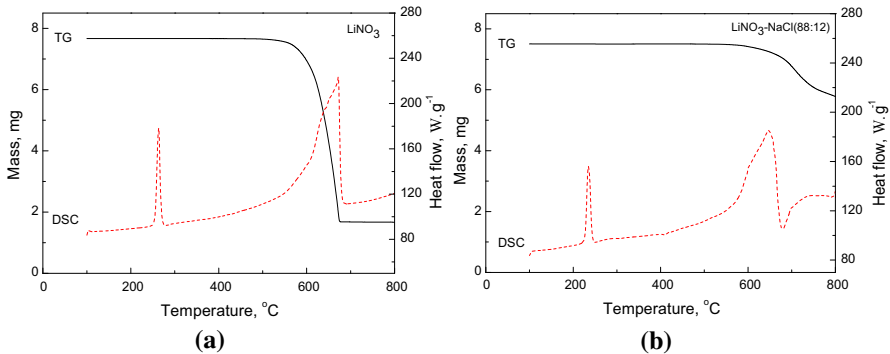
## 3.4 Specific Heat of LiNO$_3$–NaCl PCM

The specific heat of PCM is an important parameter for sensible heat storage. Because the materials need to experience the phase change transformation from solid phase to liquid phase, the specific heat is divided into solid and liquid. The test results are shown in Fig. 5 and Table 4.

It can been seen that the specific heat changed little with the temperature. The average specific heats of LiNO$_3$ are 0.993 J·g$^{-1}$·°C$^{-1}$ at 150–200 °C and 1.011 J·g$^{-1}$·°C$^{-1}$ at 300–350 °C. For 88 wt% LiNO$_3$–12 wt% NaCl, the specific heats are 1.064 J·g$^{-1}$·°C$^{-1}$ and 1.016 J·g$^{-1}$·°C$^{-1}$ at the same temperature range. Their specific heats are higher than those of the others. The specific heat of 80 wt% LiNO$_3$–20

**Table 4** Average specific heat of LiNO$_3$–NaCl at different temperature ranges

| Mass rate | Average specific heat (J·g$^{-1}$·°C$^{-1}$) | |
|---|---|---|
| | 100–150 °C | 300–350 °C |
| 100:0 | 0.971 | 1.011 |
| 94:6 | 0.918 | 0.842 |
| 88:12 | 0.979 | 1.016 |
| 80:20 | 0.748 | 0.778 |



**Fig. 6** High-temperature TGA/DSC curves. (a) LiNO$_3$, (b) LiNO$_3$–NaCl (88:12)

wt% NaCl is the lowest about 0.8 J·g$^{-1}$·°C$^{-1}$. The specific heat may be related to the degree of crystallization.

## 3.5 High-Temperature Heat Stability Test

High temperature thermal stability test was done for LiNO$_3$ and 88 wt% LiNO$_3$–12 wt% NaCl. Test results are shown in Fig. 6. It can be seen that the phase change temperature of LiNO$_3$ is 255 °C, and the melting endothermic peak appears at around 262 °C. TG curve of corresponding temperature is horizontal, which illustrates that there is no thermal decomposition. The material has good thermal and chemical stabilities. With the increase in temperature, LiNO$_3$ starts to decompose at around 560 °C, and the mass of LiNO$_3$ decreases about 10 % at 600 °C. The mass of LiNO$_3$ falls rapidly when the temperature is above 600 °C. The decomposition reaction almost ends at 675 °C.

The phase change temperature of 88 wt% LiNO$_3$–12 wt% NaCl is 223.6 °C, and the melting endothermic peak appears at about 235 °C. The TG curve remains level during the molten salt endothermic melting process. It illustrates that the material is stable. With further increase in the temperature, TG curve still tends to level until 600 °C. The mixed molten salt begins to decompose at about 620 °C, which increases about 60 °C than pure LiNO$_3$. When the temperature reaches 667 °C, the mass of the sample decreases by 5 %. The decomposition reaction is shown in Eq. 1.

$$LiNO_3 \rightarrow Li_2O + NO_2 + O_2 \tag{1}$$
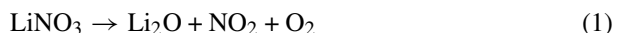
Comparing $LiNO_3$ and 88 wt% $LiNO_3$–12 wt% NaCl, $LiNO_3$ can be applied under 560 °C and 88 wt% $LiNO_3$–12 wt% NaCl can be applied below 620 °C. Adding a small amount of NaCl will obviously increase the decomposition temperature and application scope of $LiNO_3$.

## 4 Conclusion

$LiNO_3$–NaCl with different mass ratio was prepared, tested and analyzed. 88 wt% $LiNO_3$–12 wt% NaCl with the best eutectic point is specifically analyzed. The components, crystalline state and thermal stability were tested and studied. The main conclusions are as follows:

1.  XRD test shows that the peak intensity difference of NaCl and $LiNO_3$ is the smallest in the two groups of (200) and (104), (220) and (113) for the sample of 88 wt% $LiNO_3$–12 wt% NaCl. It illustrates that it has the best mutual melting and crystallization effect in all the tested samples.
2.  Some regular multilateral cube structure attaches to crystal bed surface for the samples of 94 wt% $LiNO_3$–6 wt% NaCl and 80 wt% $LiNO_3$–20 wt% NaCl. The crystal surface is relatively smoother, and no other exposed crystal structure can be seen for 88 wt% $LiNO_3$–12 wt% NaCl. The element position distribution is analyzed through EDS. It can be concluded that the main component of the regular multilateral cube is NaCl. NaCl and $LiNO_3$ mutually melt at 88 wt% $LiNO_3$–12 wt% NaCl ratio, and it achieves the best crystallization effect in all the samples.
3.  Because of heterogeneous nucleation effect, the addition of NaCl decreases the phase change temperature. For 88 wt% $LiNO_3$–12 wt% NaCl, the phase change temperature decreases 31 °C and the melting phase change latent heat increases 27.1 $J \cdot g^{-1}$ than that for pure $LiNO_3$. The latent capacity increases by about 7.5 %. The addition of NaCl improves the performance of $LiNO_3$. The specific heats of $LiNO_3$ and 88 wt% $LiNO_3$–12 wt% NaCl are higher than that of the others. This may be related to the crystallization degree.
4.  The result of high-temperature thermal stability test shows that $LiNO_3$ can be used under 560 °C and 88 wt% $LiNO_3$–12 wt% NaCl can be used below 620 °C. The addition of NaCl extends the applicable scope of $LiNO_3$.

## References

1.  T.X. Li, R.Z. Wang, J.K. Kiplagat, Y.T. Kang, Energy **50**, 454 (2013)
2.  D. Zhou, P. Eames, Sol. Energy Mater. Sol. Cells **167**, 157 (2017)
3.  M.M. Kenisarin, Sol. Energy **107**, 553 (2014)
4.  S. Wu, T.X. Li, T. Yan, Y.J. Dai, R.Z. Wang, Int. J. Heat Mass Transf. **102**, 733 (2016)
5.  X. Xiao, P. Zhang, M. Li, Energy Convers. Manag. **105**, 272 (2015)
6.  A.F. Elmozughi, L. Solomon, A. Oztekin, S. Neti, M. Guglielmi, G. Brusatin, Int. J. Heat Mass Transf. **78**, 1135 (2014)
7.  T.X. Li, J.H. Lee, R.Z. Wang, Y.T. Kang, Energy **55**, 752 (2013)

8.  M.M. Kenisarin, Renew. Sustain. Energy Rev. **14**, 955 (2010)
9.  G.A. Lane, Sol. Energy Mater. Sol. Cells **27**, 135 (1991)
10. R. Pilar, L. Svoboda, P. Honkova, L. Oravova, Thermochim. Acta **546**, 81 (2012)
11. P.D. Myers, D.Y. Goswami, Appl. Therm. Eng. **109**, 889 (2016)
12. N. Arconada, L. Arribas, B. Lucio, J. González-Aguilar, M. Romero, Sol. Energy **167**, 1 (2018)
13. Y.Y. Yang, J. Luo, S.H. Li, G.L. Song, Y. Liu, G.Y. Tang, Sol. Energy Mater. Sol. Cells **139**, 88 (2015)
14. M. Liao, J. Ding, X.L. Wei. Inorganic Chemicals Industry **40**, 15 (2008) [**in Chinese**]
15. A.M. Gasanaliev, B.Y. Gamataeva, Russ. Chem. Rev. **69**, 179 (2000)
16. Q. Peng, X.X. Yang, J. Ding, Appl. Energy **112**, 682 (2013)
17. R. Tamme, T. Bauer, J. Buschle, Int. J. Energy Res. **32**, 264 (2008)
18. G.Z. Xu, G.H. Leng, C.Y. Yang, Y. Qin, Y.T. Wu, H.S. Chen, L. Cong, Y.L. Ding, Sol. Energy **146**, 494 (2017)
19. Y. Li, P. Li, Q.Z. Zhu, Q.F. Li, Int. J. Thermophys. **37**, 103 (2016)
20. Y. Li, P. Li, Q.Z. Zhu, Y.M. Yu, J. Chin. Ceram. Soc. **46**, 624 (2018). [**in Chinese**]
21. C.Y. Zhao, Z.G. Wu, Sol. Energy Mater. Sol. C. **95**, 3341 (2011)
22. L.P. Drouot, M.J. Hillairet, J. Sol. Energy **106**, 83 (1984)
23. G.Y. Liu, Dissertation for Master's Degree (Shanghai University of Electric Power, 2018) [**in Chinese**]
24. M.G. Broadhurst, J. Chem. Phys. **36**, 2578 (1962)
25. J. Xu, Y. Ma, W. Hu, M. Rehahn, G. Reiter, Nat. Mater. **8**, 348 (2009)